Submitted to Metallurgical Transactions

RECEIVED
LAWRENCE
RADIATION LABORATORY

FEB 9 1971

LIBRARY AND
DOCUMENTS SECTION

UCRL-20348
Preprint c. 2

FRACTURE AND FRACTOGRAPHY OF METASTABLE AUSTENITES

W. W. Gerberich, P. L. Hemmings,
V. F. Zackay

December 1970

AEC Contract No. W-7405-eng-48

TWO-WEEK LOAN COPY

This is a Library Circulating Copy which may be borrowed for two weeks. For a personal retention copy, call Tech. Info. Division, Ext. 5545

UCRL-20348 c. 2

LAWRENCE RADIATION LABORATORY
UNIVERSITY of CALIFORNIA BERKELEY

25

DISCLAIMER

This document was prepared as an account of work sponsored by the United States Government. While this document is believed to contain correct information, neither the United States Government nor any agency thereof, nor the Regents of the University of California, nor any of their employees, makes any warranty, express or implied, or assumes any legal responsibility for the accuracy, completeness, or usefulness of any information, apparatus, product, or process disclosed, or represents that its use would not infringe privately owned rights. Reference herein to any specific commercial product, process, or service by its trade name, trademark, manufacturer, or otherwise, does not necessarily constitute or imply its endorsement, recommendation, or favoring by the United States Government or any agency thereof, or the Regents of the University of California. The views and opinions of authors expressed herein do not necessarily state or reflect those of the United States Government or any agency thereof or the Regents of the University of California.

FRACTURE AND FRACTOGRAPHY OF METASTABLE AUSTENITES

*W. W. Gerberich, †P. L. Hemmings, *V. F. Zackay

*Inorganic Materials Research Division, Lawrence Radiation Laboratory, Department of Materials Science and Engineering, College of Engineering, University of California, Berkeley, California

†Kaiser Aluminum and Chemical Corporation, Pleasanton, California

ABSTRACT

Variations of external test variables such as rate and temperature, and changes in alloy composition are shown to have a number of effects on the fracture of high-strength, metastable austenitic steels. An unusual rate-dependent, fracture mode transition is explained in terms of an adiabatic heating effect at the crack tip. The normally severe thickness transition is much less pronounced in metastable austenites due to the large energy dissipation associated with the invariant shear of the strain-induced martensite transformation. Fractographically, it was ascertained that at room temperature, both phases failed in a ductile manner, but at -196°, martensite containing greater than about 0.27 wt % carbon would cleave. This resulted in a "ductile-brittle" transition in metastable austenites at -196°C as a function of carbon content. Other compositional variations may change the austenite stability which controls the amount of strain-induced martensite occurring at the crack tip. It is shown that a plane stress fracture toughness (K_C) approaching 500,000 psi-in.$^{1/2}$ may be achieved by decreasing the stability of the austenite. The variation of K_C with austenite stability qualitatively verifies a theoretical model for the invariant shear contribution to the fracture toughness of metastable austenites.

INTRODUCTION

Over the last decade, it would appear that a plateau has been reached with respect to the strength-toughness combinations in ultra high-strength steels. For example, 18 Ni-maraging steels are limited to plane strain fracture toughness levels near 120 ksi-in$^{1/2}$.[1,2] Although some high strength, 12 Ni-maraging steels and 9 Ni-4 Co-0.25 C steels have exceeded this value, these have generally had yield strengths somewhat below 200,000 psi.[1-3] Similarly, for thin sheet, it has been difficult to obtain plane stress fracture toughness levels over 300,000 psi-in$^{1/2}$ for materials with yield strengths greater than 200,000 psi.[3]

One possibility of markedly exceeding these plateaus is utilization of the strain-induced phase transformation as an energy dissipation mechanism at the tip of a crack.[4,5] Specifically, in metastable austenites that had previously been warm-worked above M_D to produce yield strengths in excess of 200,000 psi, the austenite to martensite phase transformation provides an array of interesting mechanical properties.[5-8] Preliminary results[5,8] had indicated that relatively high toughness could be achieved in both thin sheet and thick plate.

The present study is an extension of the earlier investigations and has the following objectives: (1) A quantitative study of an unusual fracture transition phenomenon which was strain rate dependent. (2) A more detailed exploration of the dependence of the fracture morphology as a function of composition and testing temperature. (3) Further verification of a proposed theoretical fracture model by variation of austenite stability through composition controls. By such means the amount of strain induced phase appearing at the crack tip can be systematically varied.

MATERIALS AND PROCEDURES

The steels utilized in this study are modifications of those reported by Gerberich et al.[5,8] Variations in composition, principally in Cr, Ni and Mo, provide a range of chemical stabilities with respect to the strain-induced phase transformation. Because the carbon content is a major variable influencing fracture morphology and plane strain fracture toughness the steels of Table I are listed in the order of increasing carbon contents. Steel F was produced by the Crucible Steel Corporation in the form of 7-inch wide by 36-inch long sheets. It was estimated that the average temperature of prior deformation for this steel was about 370°C. All other steels were produced in a laboratory mill according to procedures given by Zackay, et al.[6] The only deviations here were that the plates were austenitized at 1200°C to provide maximum solution of prime carbides and an ice-brine quench was utilized to minimize alloy segregation during cooling. In addition, where very thick sections were involved, e.g. for making one-inch thick plate, upset forging was desirable to avoid splitting during subsequent rolling operations.

Uniaxial tensile and fracture toughness testing methods were identical to those utilized previously[5,8] for the evaluation of high-strength, metastable austenites. In general, this entailed either single-edge-notch (SEN) or center-notched specimens for evaluation of plane stress (K_C) conditions and crack-line loaded specimens for plane strain (K_{IC}) estimates. The only other type of measurement was that of a secant offset estimate of K_{IC}, according to ASTM[9] standards.

The quality of the thick plate utilized in this investigation

varied somewhat with processing conditions and composition. A prior deformation treatment of 80 percent requires a starting billet 2-1/2 to 5 inches thick. Deformation of the billets at 450°C resulted in some edge cracking. Although alloy A was somewhat easier to roll than the other alloys and this did not occur, some cracking did appear in alloys B, G and H. As a consequence of this edge cracking there were some slightly premature failures in the tensile tests which were taken from the plate edges. However, in the crack-line loaded samples, where the pre-crack was located in the center of the plate, there was little degradation of properties.

For evaluation of the microscopic fracture mode, standard two-step plastic-carbon replication was utilized for electron fractography. Shadowing with platinum-palladium at an angle of about 45 degrees provided additional contrast. A non-standard etching reagent of 5 grams of cupric-chloride in 100 cc each of water, HCl and methyl alcohol was utilized to etch the martensitic regions of some of the fracture surfaces before replication. This reagent did not appreciably etch the austenitic regions so that the two phases could be differentiated on this basis. Also, a limited amount of scanning electron microscopy of the fracture surfaces was accomplished with a JEOL model JSM-1 operating in the secondary electron mode at 25KV.

RESULTS AND DISCUSSION

A STRAIN RATE DEPENDENT FRACTURE TRANSITION

It was pointed out previously[5] that there was an unusual fracture mode transition in metastable austenites in that extensive slow crack growth occurred entirely in a flat mode while rapid fracture occurred in a shear mode. This flat crack growth mode was not a brittle fracture process as it occurred near stress intensity levels of 200 ksi-in.$^{1/2}$ and electron fractography verified that the microscopic mode was microvoid coalescence. This unusual fracture mode was explained in terms of a two-step fracture process occurring in a material exhibiting a strain-induced phase transformation.[5] This will be discussed in a subsequent section. It was observed that the flat fracture mode transition to a shear mode depended upon the crack velocity, which is a function of the testing (crosshead) rate. It was inferred that this behavior was probably due to adiabatic heating at the crack tip. However, there was insufficient data to substantiate the validity of these limited observations. In the present study, additional data on this material (steel A) at -196°C and on D and E at room temperature verify that this rate effect is general, as seen in Fig. 1. It would also appear that there is a maximum on the stress intensity at some intermediate crosshead rate and that for crosshead rates much less than 10^{-3} in/sec, the fracture toughness decreases.

A theoretical model can be derived based upon the fact that as the crack velocity increases, the temperature build up at the crack front finally increases sufficiently so that the rate of production of strain-induced martensite decreases. If the transformation decreases sufficiently,

a fracture mode transition from flat fracture to the shear fracture would occur, since the shear mode would be characteristic of a more nearly single-phase, high-strength, ductile material. For the model, it it first necessary to describe the crack velocity in terms of the crosshead rate and secondly, to describe the maximum temperature rise around the crack, treating the crack tip as a slowly-moving, point heat source.

For the crack velocity analysis, Irwin[10] has considered a centrally-notched plate under a uniform tensile load. The testing machine speed, R, is given in terms of the length of a plate, L, with compliance, C_s, under load, P, by

$$R = \frac{dL}{dt} = C_s \frac{dP}{dt} + P \frac{dC_s}{dt} \tag{1}$$

Since the fracture mode transition occurs near maximum load where dP/dt=0, the crosshead rate is approximately

$$R \simeq P \frac{dC_s}{dt} = P\left(\frac{dC_s}{da}\right)\left(\frac{da}{dt}\right) \tag{2}$$

Irwin[10] shows further that for either constant load or fixed grip conditions, the strain energy release rate per unit thickness is given by $(P^2/2)\frac{dC_s}{d2a}$, which , in terms of stress intensity, K, is

$$K^2 = \frac{EP^2}{4}\left(\frac{dC_s}{da}\right) \tag{3}$$

where E is Young's modulus. Combining equations (2) and (3), gives the crack growth per unit thickness as

$$\frac{da}{dt} = \frac{RPE}{4K^2} \tag{4}$$

Putting this in terms of applied stress, σ_o, and taking into account the thickness leads to

$$\frac{da}{dt} = \frac{RE\sigma_o W}{4K^2} \tag{5}$$

where W, is the specimen width.

Next, an estimate of the adiabatic heating occurring as a function of test rate must be made. The maximum temperature rise about a point source, such as the tip of a crack, is based upon an analysis of the heat transfer in a plane medium. If the point source is considered to be a slowly moving crack front, the maximum temperature rise is given by[11]

$$\Delta T_{max} = \frac{\sqrt{2}\, q}{\sqrt{\pi e}\ \rho c s} \left[1 - 1/2 \left(\frac{k}{\rho c s \frac{da}{dt}} \right)^2 \right] \tag{6}$$

where ρ is the density, c is the specific heat, k is the thermal conductivity, q is the quantity of heat and s is the distance from the heat source. It was observed that about a 200°C temperature rise in tensile specimens was possible under high strain rate conditions.[12] At the tip of a moving crack, where the volume of material undergoing plastic deformation is relatively small compared to a tensile test, such a temperature build up might not be experienced. Nevertheless, it is assumed that about a 100°C rise is possible, which would be sufficient to significantly alter the rate of production of the strain-induced phase transformation. Obviously, this would be localized near the crack tip but if it occurred over some microstructural unit, s, involved in the fracture process, it would still be sufficient to cause a fracture mode transition. From metallographic sectioning of fracture surfaces,

it had been observed that the region of severe martensite production and local delamination* was limited to a region about 0.002 to 0.006 inches deep for a -196°C test and about 0.010 to 0.015 inches deep for a room temperature test.[13] For these same tests, calculation of the crack tip displacement, $2V_c$, gave values of 0.0011 and 0.0059 inches. Thus, as a first approximation, two times the crack-tip displacement might be a numerically reasonable estimate of this critical fracture region. For the thin plates under consideration, this would be given by

$$s \sim 4V_c \sim \frac{2K^2}{\sigma_{ys}E} \tag{7}$$

where σ_{ys} is the yield strength.

As an estimate of q for the material of this investigation was not available, a rough approximation was made by taking the value determined by Schonert and Weichert[11] for a rapidly growing crack in mild steel. Their empirical equation is given by

$$q = \left[0.055-0.00927 \ln\left(\frac{da/dt}{C_1}\right)\right] \text{BTU/IN}^2 \tag{8}$$

where C_1 is a constant of 118 in/sec. Values for k and c were determined from data for similar compositions of Fe-Cr-Ni-C alloys available from Kittell[14] and Smithells.[15] Considering an ambient temperature of 77°K and a temperature rise of about 100°C, the average values of k and c in the critical region were estimated to be 2.8×10^{-4} BTU/in/°C and 0.191 BTU/Lb/°C for alloy A. Combining equations (6), (7) and (8), it is seen that there is a stress intensity factor for which a maximum temperature rise is attained over the critical fracture region as given by

---

* This local delamination is discussed more fully in the next section.

$$K^2 = \frac{\sigma_{ys} E\ C_2}{\rho c \Delta T_{max}} \left[1 - 0.168 \ln\left(\frac{RE\sigma_o W}{4K^2 C_1}\right)\right]\left[1 - \left(\frac{k}{\rho c} \cdot \frac{\sigma_{ys}}{2R\sigma_o W}\right)^2\right] \quad (9)$$

where C_2 is a constant of 0.0133 BTU/IN^2. The stress intensity may be calculated by iteration, and for this purpose equation (9) may be rewritten as

$$\frac{K^2}{A(1-D^2)} + 0.168 \ln\left(\frac{B}{K^2}\right) = 1 \quad (10)$$

with $A = \frac{\sigma_{ys} E C_2}{\rho c \Delta T_{max}}$; $B = \frac{RE\sigma_o W}{4C_1}$; $D = \frac{\sigma_{ys} K}{2R\sigma_o W \rho c}$.

The -196°C data for steel A from Fig. 1 were utilized for testing of the empirical model developed above since this was the most complete set of data. Furthermore, these were the only tests obtained on 6 inch wide, center-notch plates for which the actual crack growth rate had been measured. The yield strength for this alloy was 258,000 psi at -196°C. The remaining parameter to be established is the value of the applied stress at instability. It was observed that this varied somewhat but was about 75,000 psi ± 7,000 psi. Although this variation would normally be significant in a stress intensity calculation, because of the nature of equation (9), calculation showed this to be a negligible effect as compared to the rate effect. Thus, for simplification, σ_o was taken as a constant equal to 75,000 psi.

With the values of the constants and the material parameters as given above, it was possible to calculate stress intensity as a function of crosshead rate. This was compared to the actual stress intensity at the point of instability in Fig. 2. The agreement is reasonable with a maximum on K_C being predicted near 10^{-2} in/sec, which is very close to that observed. At the very slow crosshead rate some disagreement exists

but this may be traced to an inaccuracy of equation (5) in describing the crack velocity. Measured values of the average crack growth rate were determined over the increment of slow crack growth preceding fracture. Considering the fact that the crack is accelerating, this would give a lower bound estimate of $(da/dt)_{max}$ at the point of instability. This data is compared to values calculated from equation (5) in Fig. 3. Although the comparison is reasonable at the higher crosshead rates, the discrepancy would be at least an order of magnitude at the slowest testing speed. Since this order of magnitude shift in da/dt can explain the discrepancy at the slower crosshead rate in Fig. 2, one might consider that this approach is quantitatively quite accurate. However, the accuracy of equation (8) in describing the heat flow at the crack tip in the present material is questionable. Furthermore, the estimate of ΔT_{max} and s can only be considered accurate within a factor of two. Thus, the agreement in Fig. 2 is probably fortuitous since equally reasonable estimates of ΔT_{max} and s could have been used which would give estimates of K off by a factor of two or more. Nevertheless, this relationship qualitatively explains the effect of crosshead speed on the resulting stress intensity at the fracture mode transition produced by adiabatic heating. It is significant that the theory indicates there should be no transition below a certain crosshead rate, a fact that had been observed for alloy D[8] and has been observed by others[12,16] for alloys of similar composition.

The other testing variable which could influence the fracture behavior is the thickness transition which normally is quite severe in high strength steels. Maximum stress intensity data obtained from

steels B, C, D and G at room temperature are compared to two medium and low alloy steels in the same strength range as a function of thickness in Fig. 4. It is seen that the drop in toughness is only about one half of that normally observed for high strength steels. The reason for this high toughness in thick sections may be partially attributed to the strain-induced phase transformation. First, it has been suggested[13] that under triaxial stress conditions, the rate of production of martensite per unit strain is greater than under uniaxial conditions. Secondly, the strain-induced transformation itself is a large plastic energy dissipator[5] due to the orientation of the shape change in the direction of the macroscopic shear. The orientation of the martensite plates in the direction of the macroscopic shear is seen to be a general effect for various steels, thicknesses and test temperatures as seen in Fig. 5. These facts would tend to indicate that a larger amount of energy may be dissipated in the center of a thick plate than is normally possible without a strain-induced phase transformation. In fact, it may be difficult to approach a truly plane strain condition in these materials. The exception to this is discussed in the following section.

FRACTURE MORPHOLOGY AS A FUNCTION OF TESTING VARIABLES

In the present study, a ductile-brittle transition was observed with respect to fracture in the strain-induced phase as a function of test temperature. As this transition was dependent upon the carbon concentration, the discussion of fracture morphology will be in two parts: for steels with carbon levels from 0.20 - 0.24 wt. percent and for steels with 0.27 - 0.35 wt. percent C.

First, consider the relatively stable alloy A which, at room

temperature, exhibits relatively little strain induced-phase transformation. In Fig. 6, it is seen that completely dimpled rupture occurs on the fracture surface, which is characteristic of the fracture in austenite. On the other hand, the same steel fractured at -196°C shows two distinct modes of rupture as seen in Fig. 7. The fairly large shear dimples on the order of two microns in size are representative of fracture in austenite while the very small dimples, which seem to be oriented along a series of fine bands in the lower right of Fig. 7(b), are characteristic of martensite fracture. These regions were verified to be martensitic as they were etched by the reagent prior to making the replica. In between these major regions, a stretched region is noted as seen in the upper left corner of Fig. 7(a) and in the middle of Fig. 7(b). It may also be noted that the dimples in the austenite next to the stretched regions were oriented perpendicular to the stretched bands.

The morphological factors described above can be more clearly seen in a composite of a similar region, as shown in Fig. 8. As can be seen from upper left to lower right there are alternating regions of dimpled rupture in the austenite, a stretched region, fracture in martensite, another stretched region, and, finally, dimpled rupture in austenite. This fracture morphology was explained[5] in terms of the martensite fracturing first, followed by a tearing in the austenite regions in between, the result being that local fracture in austenite was perpendicular to the macroscopic crack growth direction. Additional clarification of this fracture mechanism was obtained with scanning electron microscopy of a similar specimen that had not been etched. A series of magnifications of one area in Fig. 9 shows the local delamination that

was indicated in Fig. 5. Here, the deep furrows are about 10μ apart which is about the same as the austenitic grain size. Thus, one is tempted to say that the abrupt change in fracture direction is simply due to local delamination at the grain boundary. However, as seen in Fig. 5(a), the fracture in steel A does not follow along the grain boundary and in many cases the local delamination is transgranular. In addition the detailed characteristics of these local delaminations may be matched exactly to the electron fractographic observations obtained on replicas. For example, the lower photomicrograph in Fig. 9 shows dimples, a stretched region and a martensitic fracture region from extreme right to left. These alternate regions match up to those indicated previously in Fig. 8. Hence, the deep furrows are heavily martensitic. The regular striations preceding the large furrow in Fig. 9 suggest an orderly fracture process. Since the martensite is oriented with respect to the macroscopic shear planes as seen in Fig. 5, it is possible that a repeated crystallographic slip process is responsible for the ductile fracture process in the martensite. Thus far, all of the fractographic analysis has pertained to steel A, most of it being for tests conducted at -196°C. A similar fracture transition region was observed in steel B at room temperature since the composition was sufficiently low to allow considerable martensite formation during testing. Although not so well defined, such a transition region is seen in Fig. 10 for an unetched surface.

For the higher carbon alloys, the fractographic characteristics at room temperature were similar to those observed for steel B. However, for those specimens tested at -196°C, fractography demonstrated a

distinct morphological difference. Typical micrographs from steel G, which had a K_{IC} of 67.5 ksi-in.$^{1/2}$, are shown in Fig. 11. The relatively flat featureless regions are cleavage in the martensite and on either side of these regions some very small dimples may be noted. Further investigation showed these dimples to be associated with fracture in the austenite as may be interpreted from Fig. 12. Here, a very long martensitic cleavage region is shown in the middle of these micrographs. To the left of this region there is a stretched region which is most clearly seen in the upper left hand fractograph. Immediately to the left of this are very fine shear dimples which are analogous to the shear dimples identified before as being rupture in the austenite between martensitic fracture regions. Although not perfectly obvious, these shear dimples again are oriented perpendicular to the martensitic region and hence perpendicular to the macroscopic fracture direction. Thus, the fracture process in the higher carbon steels is identical to that described above for the lower carbon steels except that at lower temperatures, e.g. -196°C, the martensite cleaves instead of tears.

Of course, this has a large effect on the fracture toughness because of the low crack propagation resistance associated with cleavage in untempered martensite. That is, as soon as the strain at the crack tip is sufficient to produce a significant amount of martensite, the martensite could cleave† and the crack could run as fast as the strain-induced phase transformation could occur. The effect of this on the plane strain fracture toughness is dramatic as is seen in Fig. 13. For

---

† This assumes that the cleavage fracture stress is less than the stress at the crack tip, i.e. the flow stress elevated by the plastic constraint factor, which is probably the case for these untempered martensites.

carbon levels less than about 0.24 wt. percent, no cleavage was observed and unusually high toughnesses were obtained at -196°C. On the other hand, where cleavage occurred for the higher carbon contents, K_{IC} values typical of tempered martensitic steels at -196°C were observed. Thus, it would seem that in order to take full advantage of the inherent toughness possible from the strain-induced phase transformation, the strain-induced phase should have a reasonable resistance to fracture.

ROLE OF AUSTENITE STABILITY IN FRACTURE

If the strain-induced phase is reasonably tough, then one should be able to enhance the fracture toughness of these materials by providing greater amounts of transformation product. This was earlier proposed by Gerberich, et al.[5] who showed that the strain-induced phase transformation is a plastic energy dissipation mechanism that is as much as a factor of five larger than the normal plastic dissipation processes occurring at a crack tip. The present study provides further confirmation of the earlier proposal. That is, as the composition varies, the degree of metastability varies and thus fracture toughness should be dependent upon some parameter which is a function of the M_D and test temperatures. The following discussion demonstrates this relationship.

It was shown[5] that the invariant shear contribution to plastic energy dissipation could be given by

$$U_{IS} = \frac{\pi}{8} B \int_0^{R_p} m \epsilon_{IS} \sigma_{\alpha'} \left(\frac{\sigma_\gamma}{E}\right)^{1/2} \left[\frac{R_p}{r} - 1\right]^{1/2} rdr \qquad (11)$$

where R_p is the plastic zone diameter, ϵ_{IS} is the invariant shear, $\sigma_{\alpha'}$ and σ_γ refer to the flow stresses of martensite and austenite, r is the distance from the crack tip and m is a transformation coefficient which is related to the alloy stability in terms of the strain-induced phase transformation. The term outside the integral is the plastic zone shape factor times the thickness while the term inside the integral represents the summation of energy density throughout the plastic zone. The transformation coefficient is a simple function of strain for these high-strength metastable austenitic steel given by[7,16]

$$V_{\alpha'} = m\epsilon^{1/2} \tag{12}$$

where $V_{\alpha'}$ is the volume fraction of martensite. Furthermore, it has been shown[7] that m may be calculated from the M_D and test temperatures so that m is directly related to the chemical free energy of the system. For a balance of the elastic energy release rate by the plastic energy dissipation rate, $\partial U_p/\partial a$, one obtains the critical stress intensity K_C to be

$$K_C = \left[\frac{\partial U_p}{\partial a} \cdot \frac{E}{B}\right]^{1/2} \tag{13}$$

Since m is a constant for any particular test and since it was determined[5] that U_{IS} was the major energy dissipation term, it may be seen from equations (11), (12) and (13) that a first approximation gives

$$K_C \propto m^{1/2} \tag{14}$$

Consider next how this relationship compares to the experimental data. Most of the data were normalized to a crosshead rate of 0.01 in./sec, e.g. see Fig. 3 for alloys D and E. The only exception was steel F

which did not reach a fracture instability at such low crosshead speeds. Therefore, data obtained at several rates on the order of 0.03 to 0.3 in./sec are reported. If an extrapolated value had been utilized, an even higher toughness would have resulted but this did not appear to be justified at this time. These data, along with several other sources,[12,16,17] show fracture toughness to be an increasing function of the transformation coefficient in Fig. 14. Considering that no plastic zone size correction was made for these estimates, these toughness levels are very high at higher values of m. Upon interpolation at values of $m = 0.5$ and $m = 2$, K_C values of 235 ksi-in.$^{1/2}$ and 460 ksi-in.$^{1/2}$ are obtained. Since $235/460 \simeq (0.5/2)^{1/2}$, it would appear that equation (14) is reasonably well followed and the theory is at least qualitatively confirmed.

In Fig. 14, there appears to be a secondary composition effect in that increasing amounts of (C+N) tend to decrease the overall level of toughness. The theoretical model developed thus far does not adequately take this into account. On a physical basis, it is an effect similar to that noted at the low temperatures where increased interstitial levels promoted cleavage. Nevertheless, it is not the same mechanism since no cleavage was noted in tests performed at room temperature.

CONCLUSIONS

1. The plane stress fracture toughness of high-strength, metastable austenites is a function of crack velocity as controlled by the adiabatic heating produced at the crack tip.
2. In order for this effect to be observed, the adiabatic temperature rise must be sufficient to significantly alter the rate of production of strain-induced martensite.
3. A theoretical model is developed to predict fracture toughness as a function of crosshead rate.
4. Fractographically, the fracture process is observed to be a two-step process with the fracture nucleating in martensitic regions and then tearing in austenitic regions between.
5. For alloys with less than 0.24 wt % C, martensite fails by a ductile fracture process; for alloys with more than 0.27 wt % C, martensite exhibits ductile fracture at room temperature but cleaves at -196°C.
6. At -196°C, a ductile-brittle transition results as a function of carbon content with low carbon alloys having plane strain fracture toughness (K_{IC}) values on the order of 140 ksi-in.$^{1/2}$ and medium carbon alloys having $K_{IC} \sim 50$ ksi-in.$^{1/2}$.
7. Plane stress fracture toughness values as high as 450 ksi-in.$^{1/2}$ were obtained.
8. The highest fracture toughness levels were achieved by making the austenite more unstable, a measure of which is the transformation coefficient, m.
9. As a first approximation, K_C is proportional to $m^{1/2}$. This qualitatively verifies the previous model which accounts for the large amount of energy plastically absorbed during the invariant shear of the transformation.

REFERENCES

1. W. S. Pellini, NRL Report 6957, (September 1969).

2. L. Raymond, Fracture: Proceedings of the Second Tewksbury Symposium, (1969), p. 241.

3. S. J. Matas, M. Hill and H. P. Munger, Metals Eng. Quart, ASM, 3, No. 3 (1963).

4. S. D. Antolovich, Trans. AIME, 242 (November 1968), p. 2371.

5. W. W. Gerberich, P. L. Hemmings, V. F. Zackay and E. R. Parker, Fracture 1969, ed. by P. L. Pratt, Chapman and Hall, Ltd., London (1969), p. 288.

6. V. F. Zackay, E. R. Parker, D. Fahr and R. Busch, Trans. Quart. ASM, 60, No. 2 (1967), p. 252.

7. W. W. Gerberich, G. Thomas, E. R. Parker and V. F. Zackay, Second International Conference on the Strength of Metals and Alloys, Asilomar, Calif. (August 1970), in press.

8. W. W. Gerberich, P. L. Hemmings, M. D. Merz and V. F. Zackay, Trans. Quart. ASM, 61, No. 4 (1968), p. 843.

9. W. F. Brown, Jr. and J. E. Srawley, Plane Strain Crack Toughness Testing of High Strength Metallic Materials, ASTM STP 410, Philadelphia (1966), p. 130.

10. G. R. Irwin, Weld. J. Res. Suppl. (November 1962), p. 519S.

11. K. Schönert and R. Weichert, Chem. Ing. Techn., 41 (1968), p. 295.

12. C. Dokko, UCRL Report 19068, University of California, Berkeley, (September, 1969).

13. W. W. Gerberich, P. L. Hemmings and V. F. Zackay, Trans. AIME, 245, (May 1969), p. 1126.

14. C. Kittel, Solid State Physics, J. Wiley and Sons, New York (1956).

15. C. J. Smithells, Metals Reference Book, Vol. II, Butterworths and Co., London (1962).

16. G. Chanani,"Fracture Characteristics of Metastable Austenitic Steels Under Cyclic Loading," Ph.D. Thesis, Univ. of Calif., Berkeley (1970).

17. W. W. Gerberich and J. Birat, Int. J. Fract. Mechanics, in press.

18. H. Bernstein and G. C. Yound, NAVORD Report 6496 (Part 21, NRL 108), Naval Research Laboratory, January 1960.

19. "Thick-Section Fracture Toughness," Report ML-TDR 64-236, Boeing-North American, Contract AF 33(657)-11461, Wright Field, October 1964.

Table 1. Chemical Compositions

Designation	Composition, Wt. %						Nominal thickness, INCHES
	C	Cr	Ni	Mo	Mn	Si	
A	0.20	13.5	8.8	3.0	2.0	1.0	0.5
B	0.24	9.0	8.0	4.0	2.0	2.0	0.5
C	0.24	9.0	7.4	4.0	2.9	2.8	0.075
D	0.26	10.1	8.8	5.5	1.7	2.0	0.08
E	0.26	9.0	9.0	4.9	2.5	2.0	0.10
F	0.27	11.2	8.0	1.9	0.4	0.1	0.10
G	0.27	9.0	7.9	4.0	1.0	2.0	1.0
H	0.28	8.8	7.9	3.9	1.0	2.0	0.5
I	0.35	9.0	8.0	4.0	2.0	2.0	0.08

Table 2. Uniaxial Tensile Data

Steel	Room Temperature Tests Yield,[a] ksi	Ultimate, ksi	Elongation,[b] %	-196°C Tests Yield,[a] ksi	Ultimate, ksi	Elongation,[b] %
A-450	182	196	9.6[c]	258	326	39
B-450	206	215[d]	25[d]	215	225[d]	8.1[d]
C-250	237	248	37	-	-	-
C-450	234	250	34	-	-	-
D-250	235	236	32	256	294[d]	13[d]
E-450	225	245	38	-	-	-
F-370	210	235	47	-	-	-
G-450	224	235[d]	24[d]	226	226[d]	9.0[d]
H-450	230	243[d]	19[d]	-	-	-
I-450	201	240	37	195	367	18

(a) Yield is associated with a yield point where sufficient strain-induced martensite forms to allow propagation of a Lüders band.

(b) Elongation in one inch except for Steel F which was in two inches.

(c) Not sufficient transformation to prevent necking.

(d) Premature failure due to microcracks formed during alloy preparation.

FIGURE CAPTIONS

1. Effect of crosshead rate on plane stress fracture toughness.
2. Theoretical prediction of crosshead rate effect.
3. Relationship between crack growth rate and crosshead rate.
4. Effect of thickness on the critical stress intensity factors for high strength metastable austenites and two commercial steels.
5. Strain-induced martensite (etched bands) near the fracture surfaces of four different metastable austenite fracture coupons.
6. Dimpled rupture in alloy A tested at room temperature where little strain-induced martensite resulted.
7. Mixed fracture mode in alloy A tested at -196°C with etched bands representing fracture in martensite and dimples representing fracture in austenite.
8. Alternating fracture regions of austenite and martensite showing local orientation of austenite fracture to be perpendicular to the macroscopic crack growth direction.
9. Scanning electron microscopy of a similar fracture surface of alloy A tested at -196°C.
10. Electron fractography of alloy B tested at room temperature.
11. Cleavage and dimpled rupture resulting in alloy G tested at -196°C.
12. Cleavage of a very long martensitic region in alloy G tested at -196°C.
13. Effect of carbon content on cleavage of martensite and, hence, on apparent K_{IC} at -196°C.
14. Influence of austenite stability on the plane stress fracture toughness of high-strength, metastable austenites. Note: All data are normalized to a crosshead rate of 0.01 in./sec except steel F where F, F', F" denote increasing crosshead speeds from 0.03 to 0.3 in./sec.

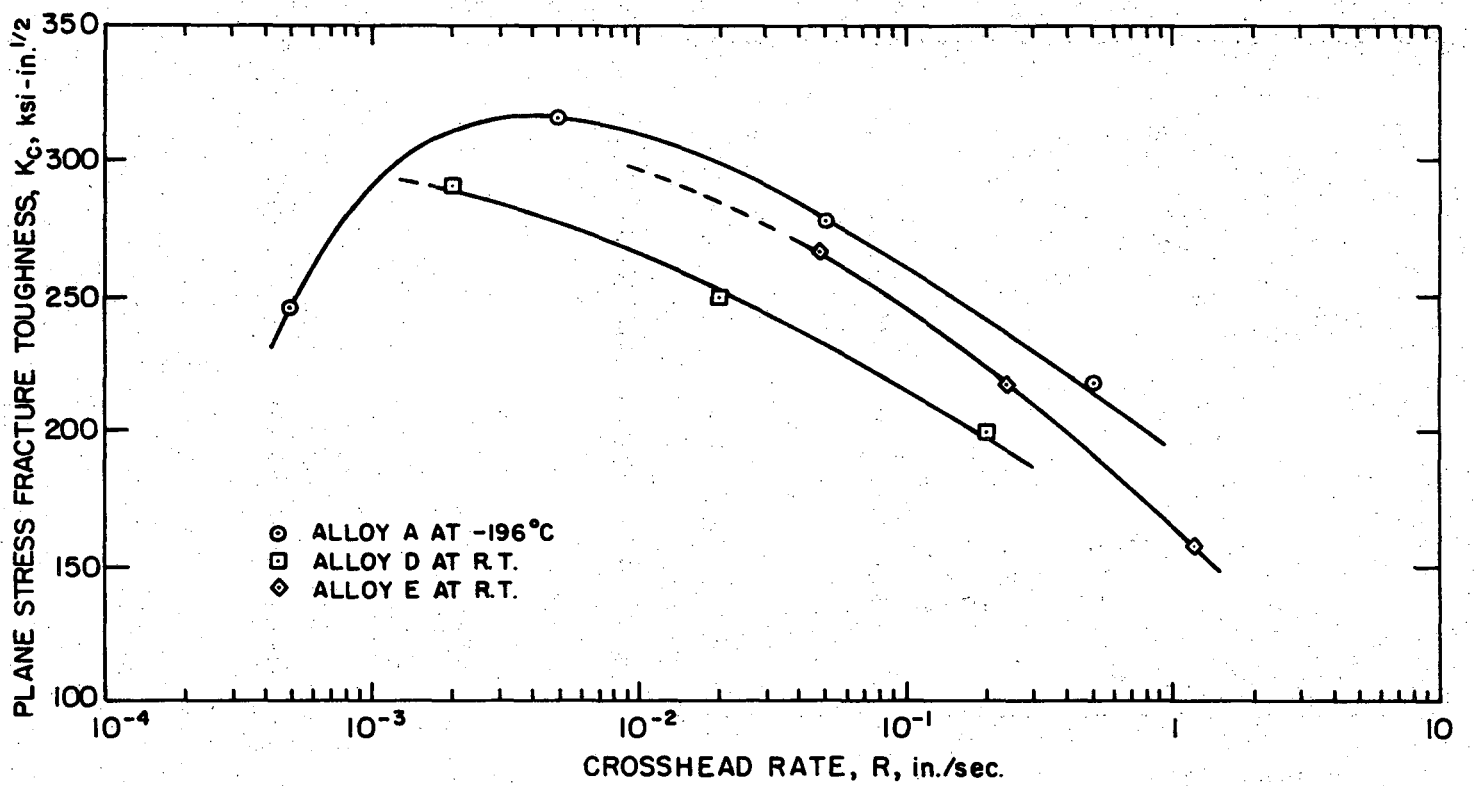

XBL 7010-6748

Fig. 1

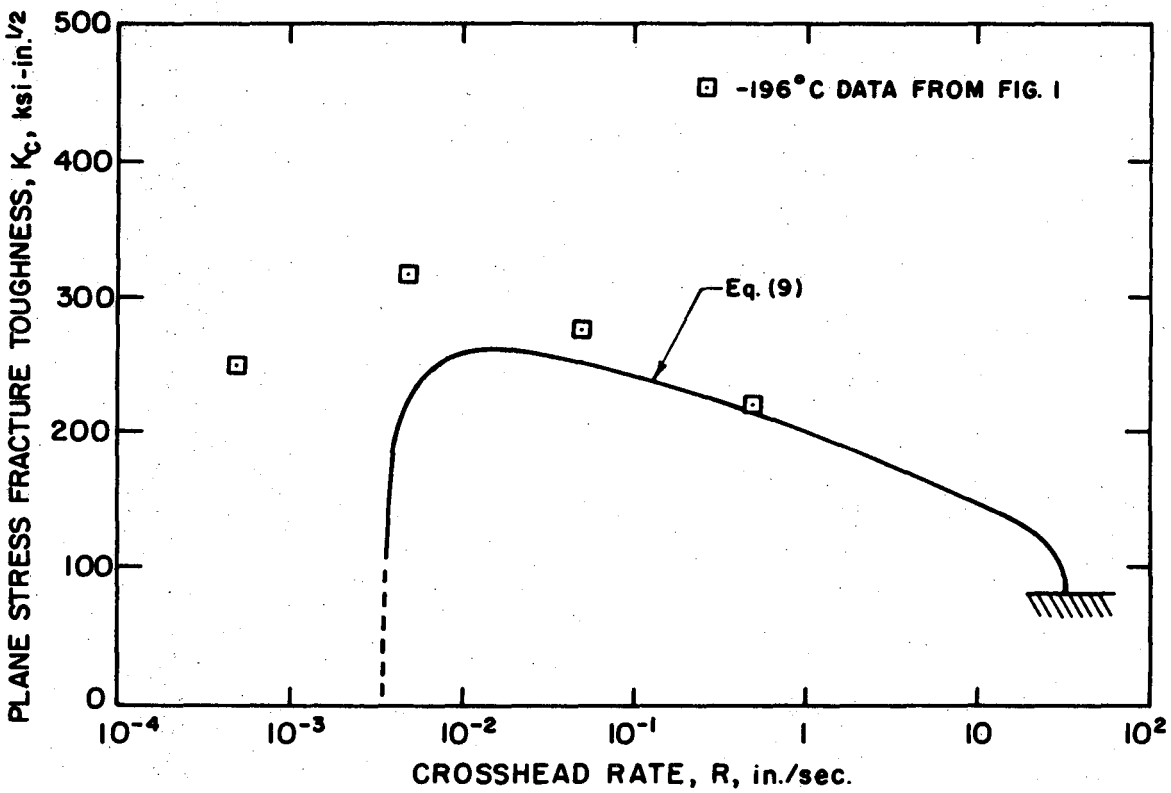

XBL 7010-6749

Fig. 2

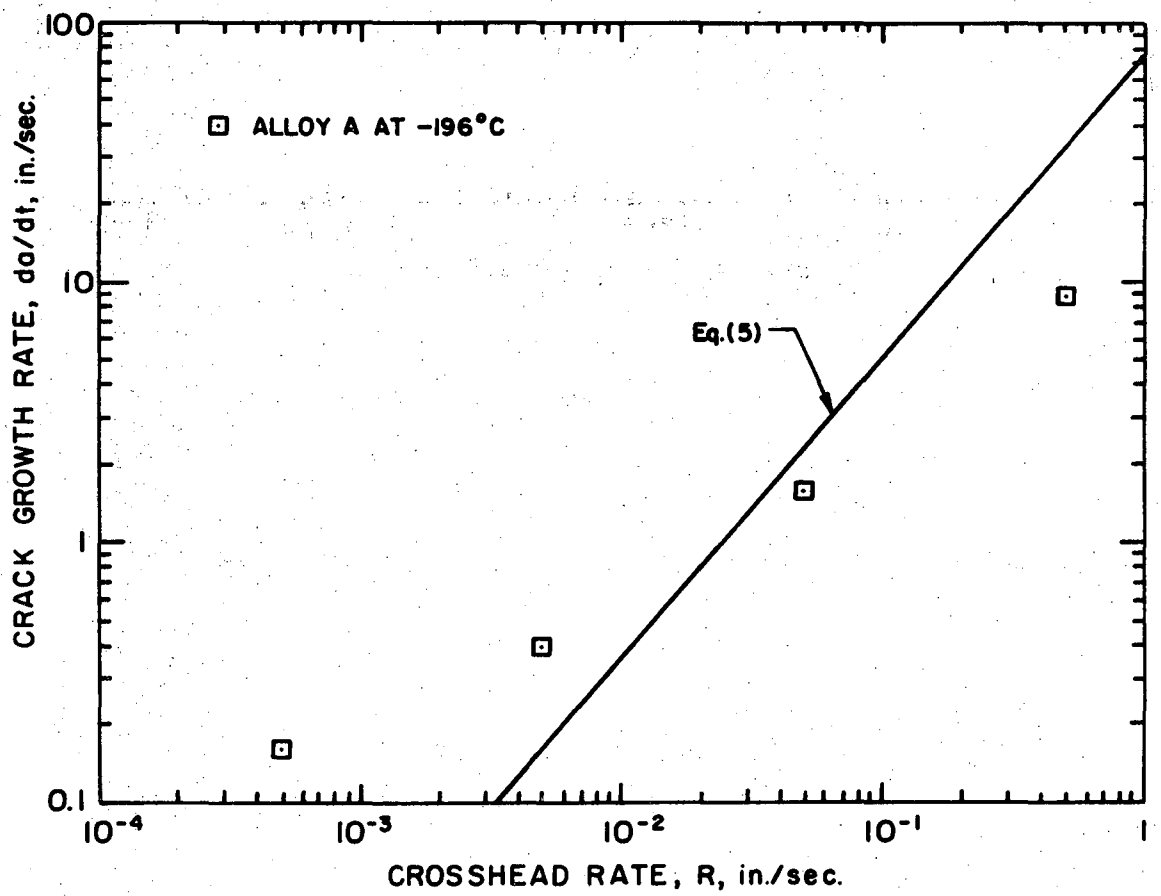

XBL 7010-6750

Fig. 3

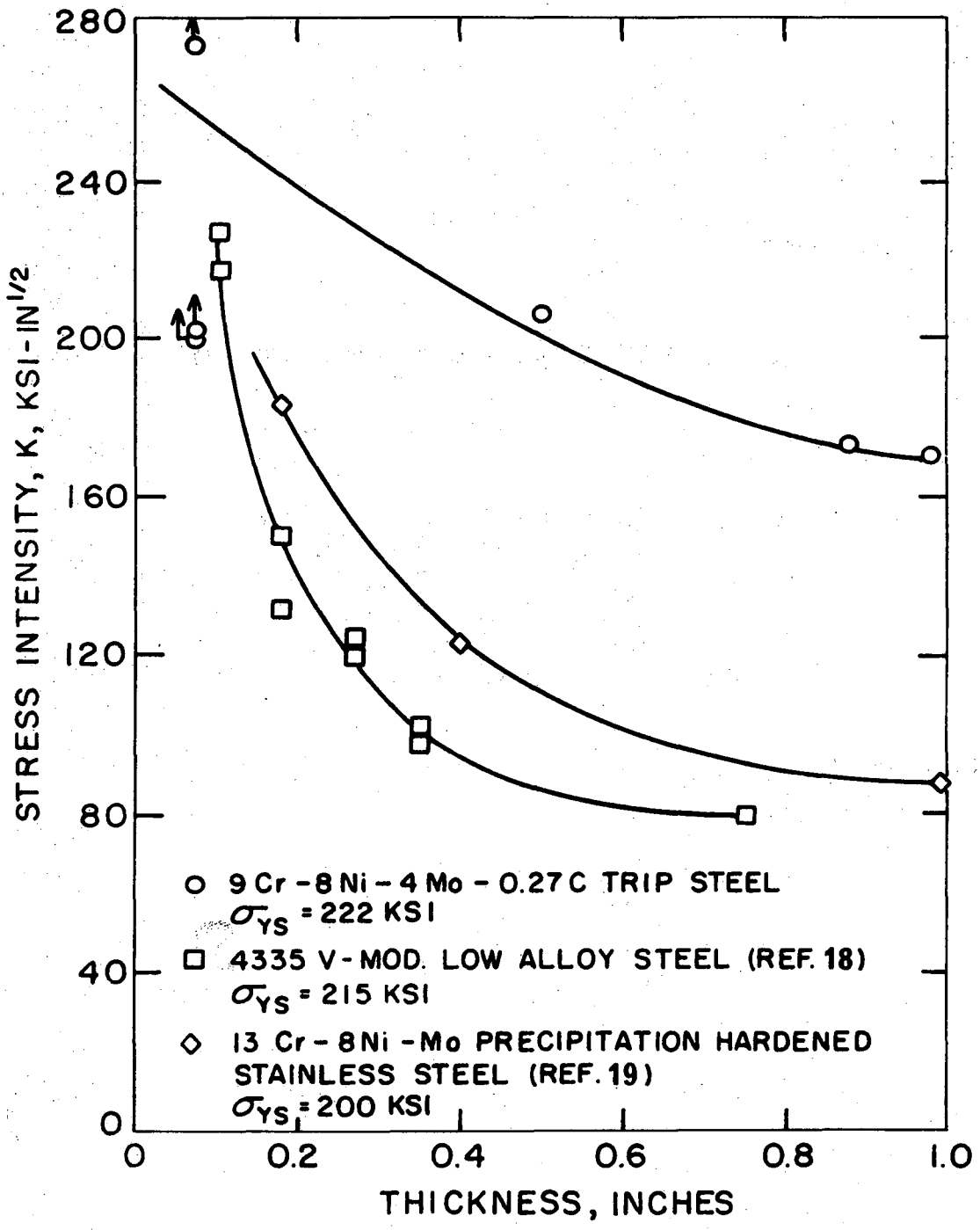

XBL 6811-6136

Fig. 4

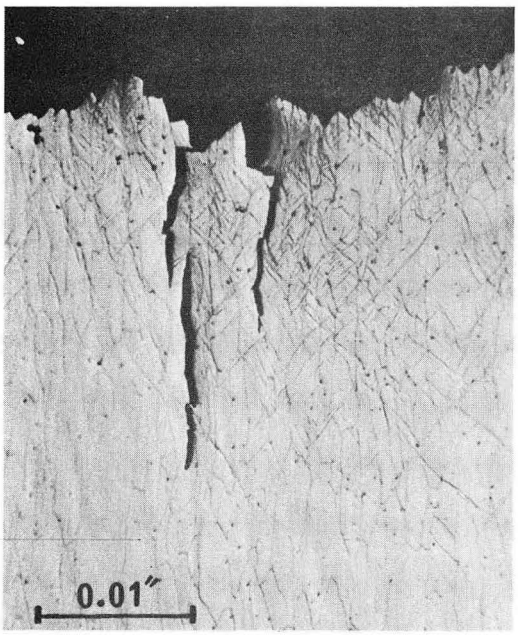

ALLOY A, -196°C TEST
0.5 IN. THICK SPECIMEN

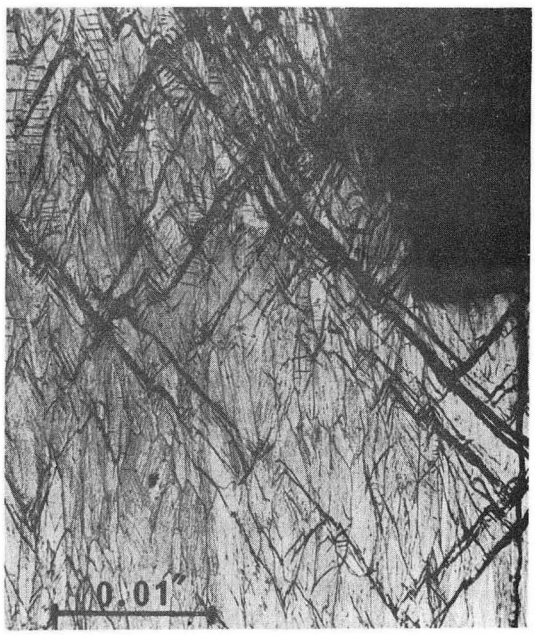

ALLOY B, R.T. TEST
0.5 IN. THICK SPECIMEN

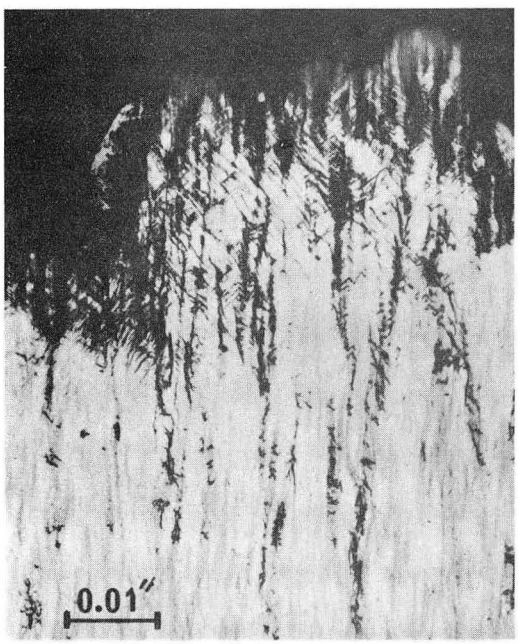

ALLOY G, -196°C TEST
1 IN. THICK SPECIMEN

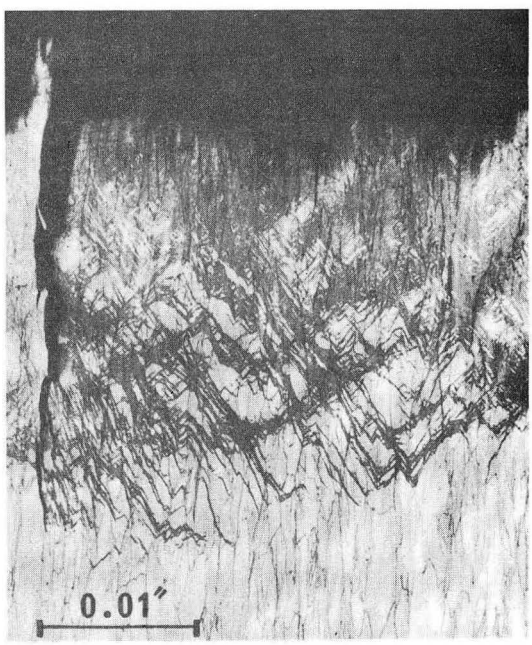

ALLOY H, -196°C TEST
0.5 IN. THICK SPECIMEN

XBB7010-4582

Fig. 5

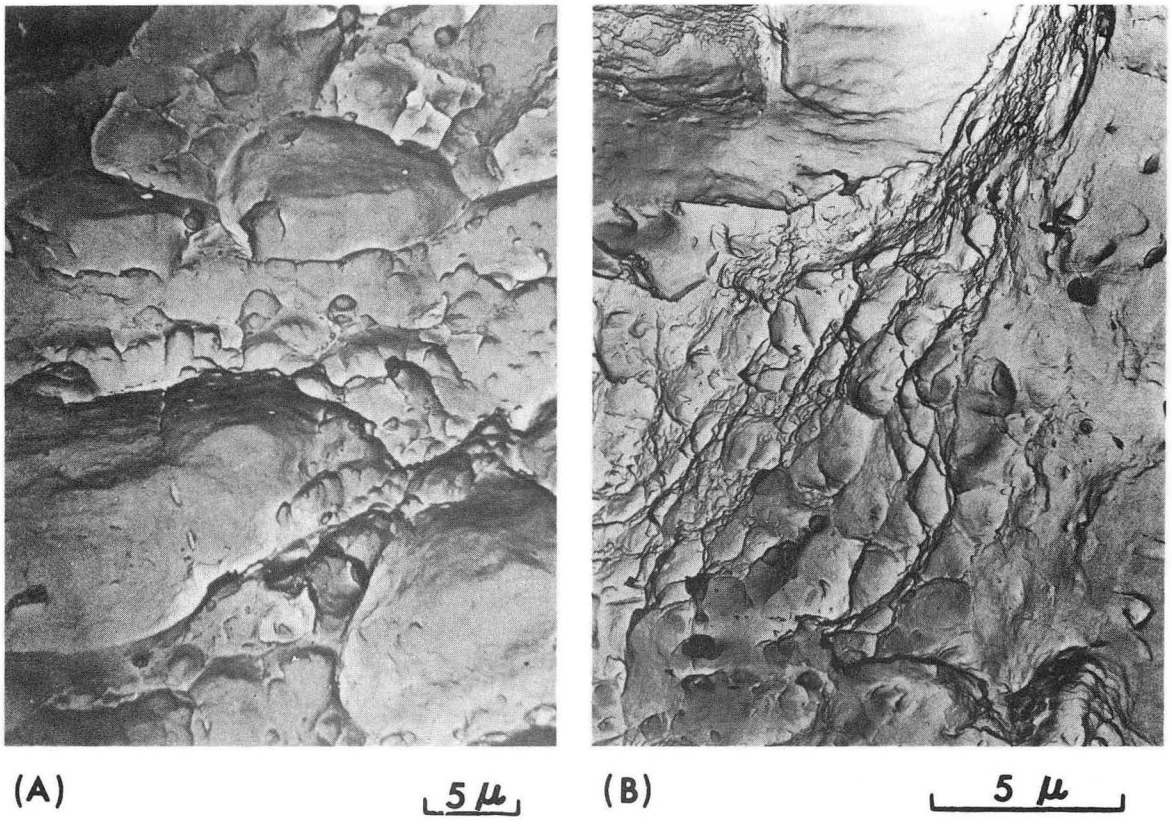

XBB7010-4581

Fig. 6

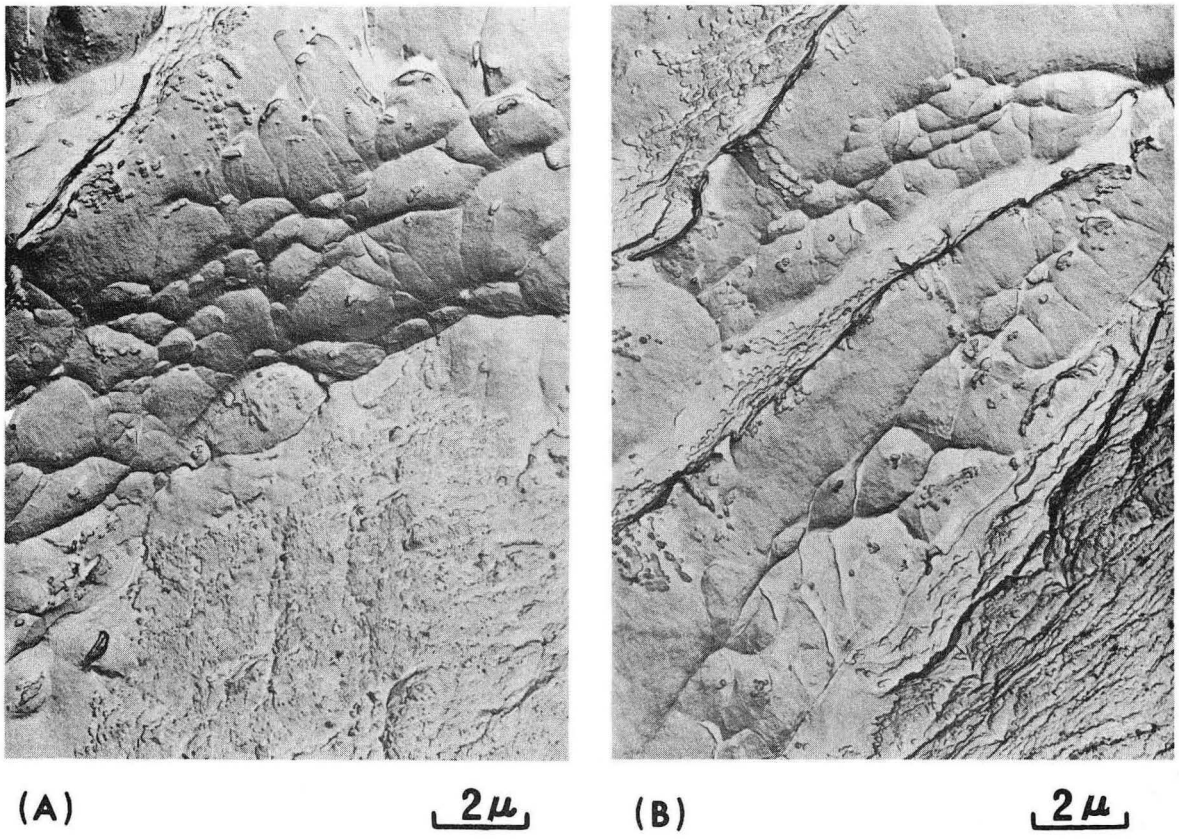

XBB689-5387A

Fig. 7

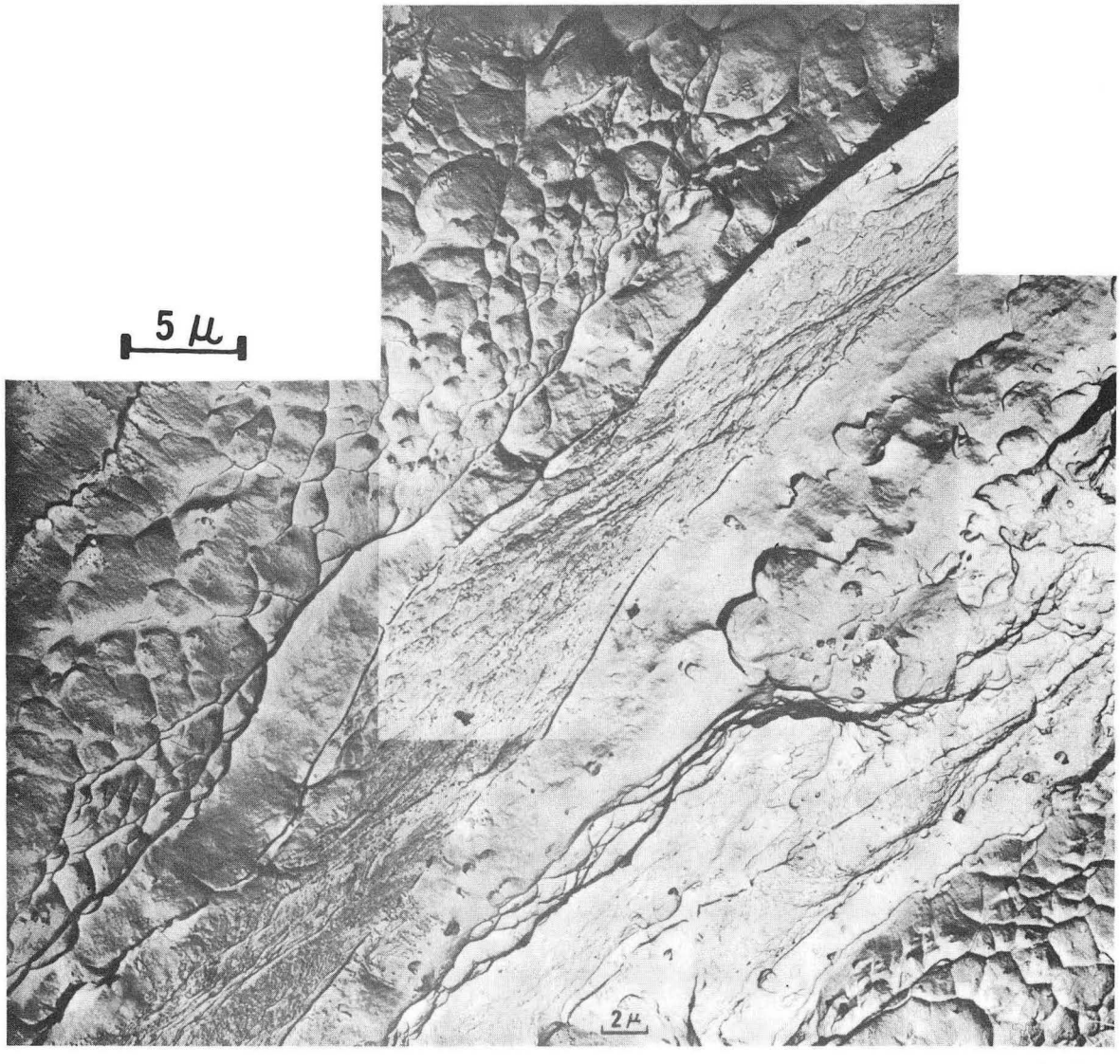

XBB7010-4580

Fig. 8

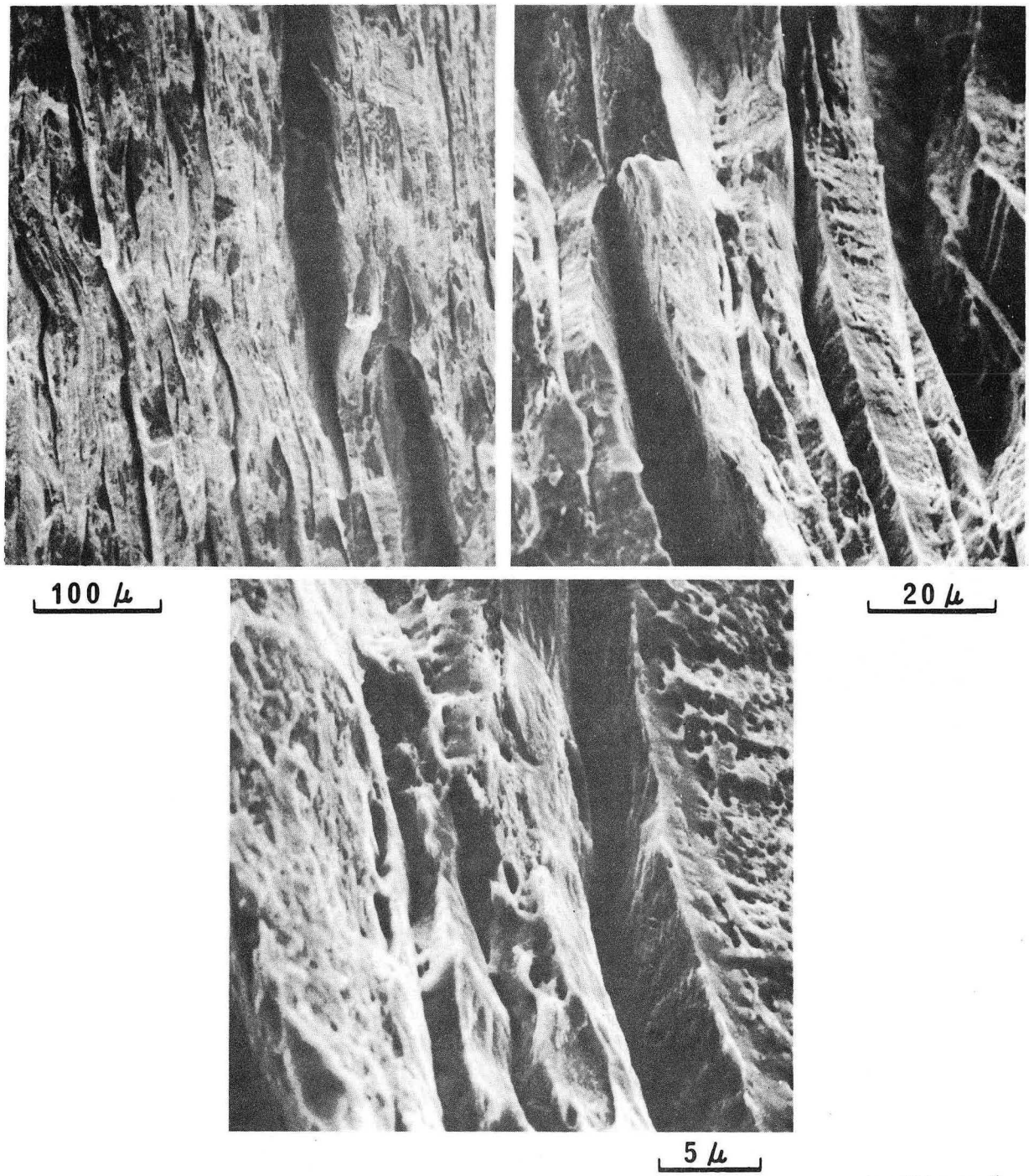

XBB701-176

Fig. 9

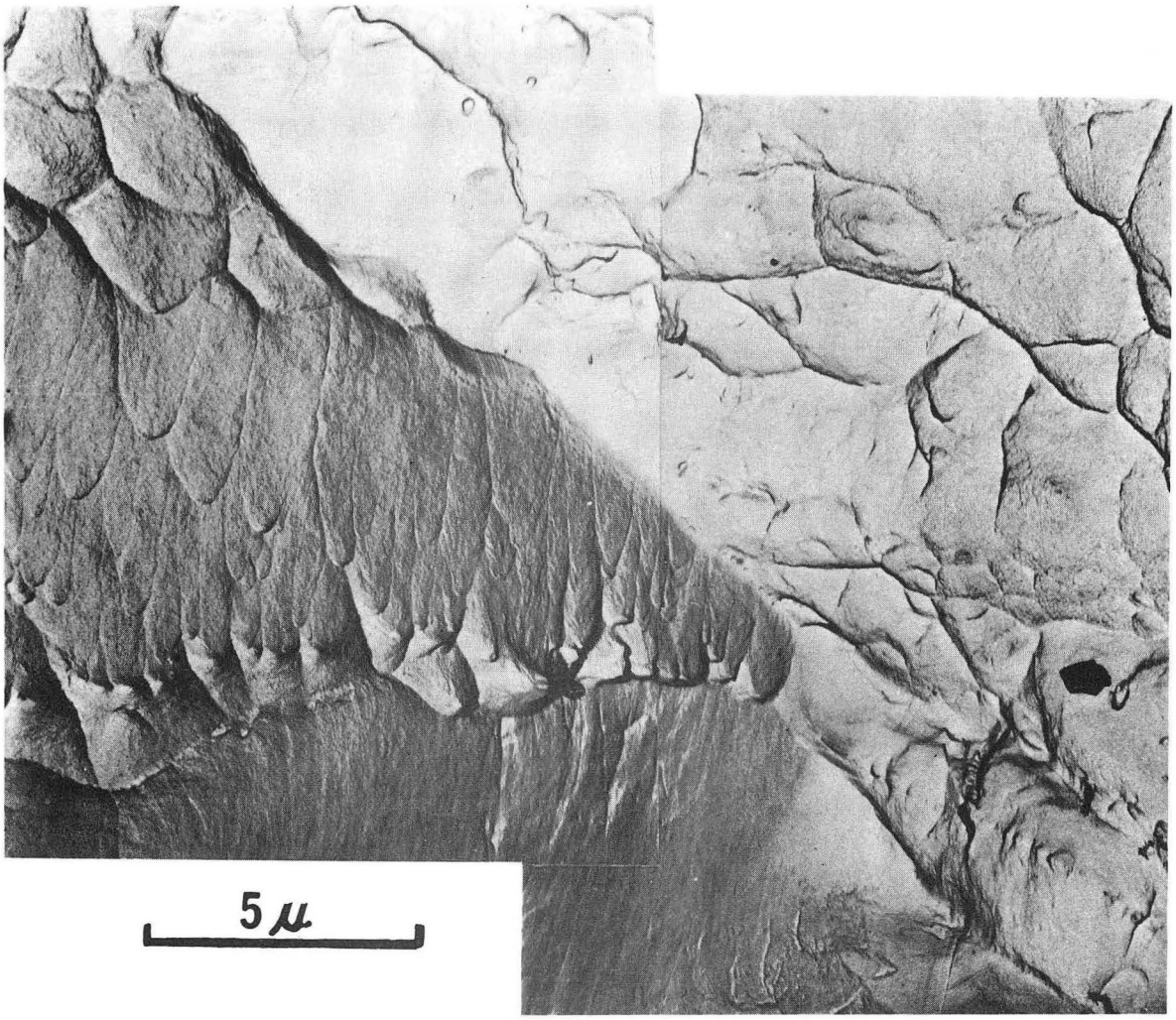

XBB7010-4579

Fig. 10

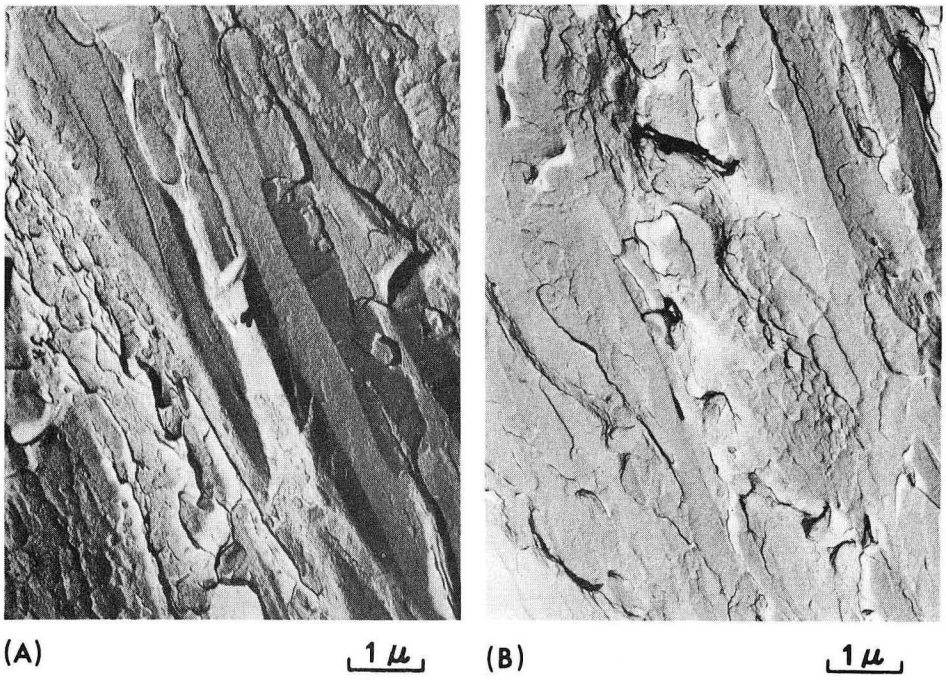

XBB701-174

Fig. 11

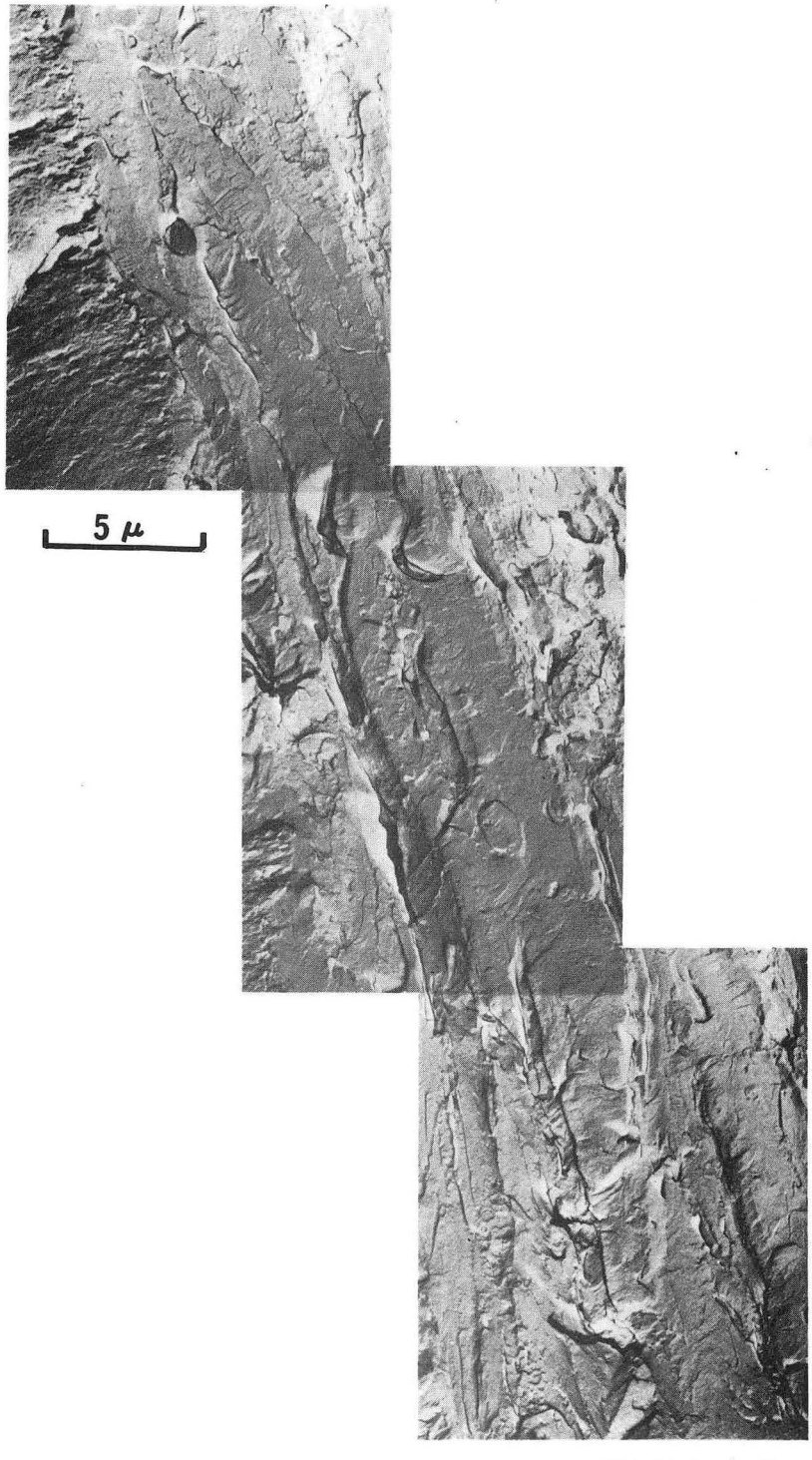

XBB7010-4583

Fig. 12

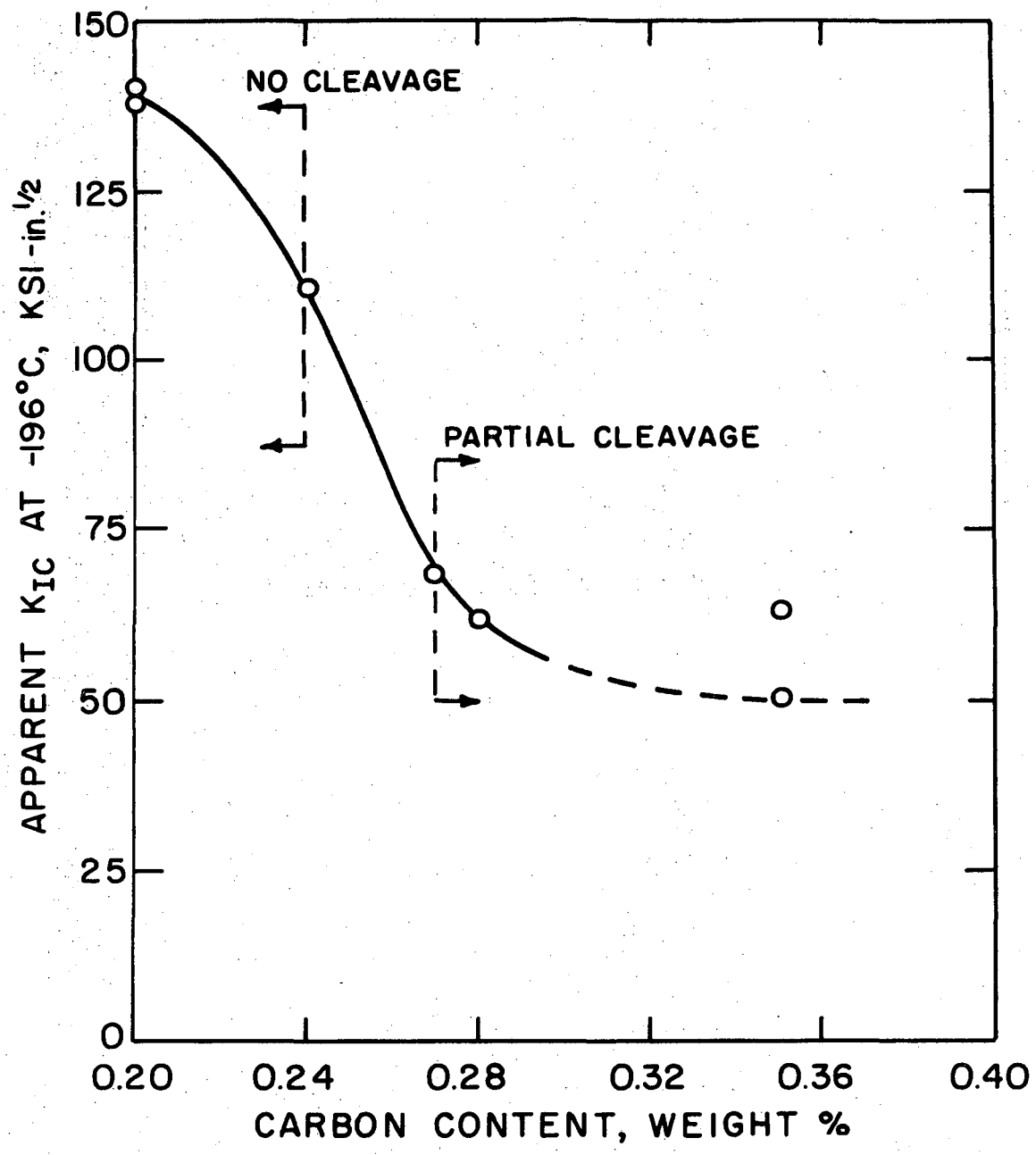

XBL 701-210

Fig. 13

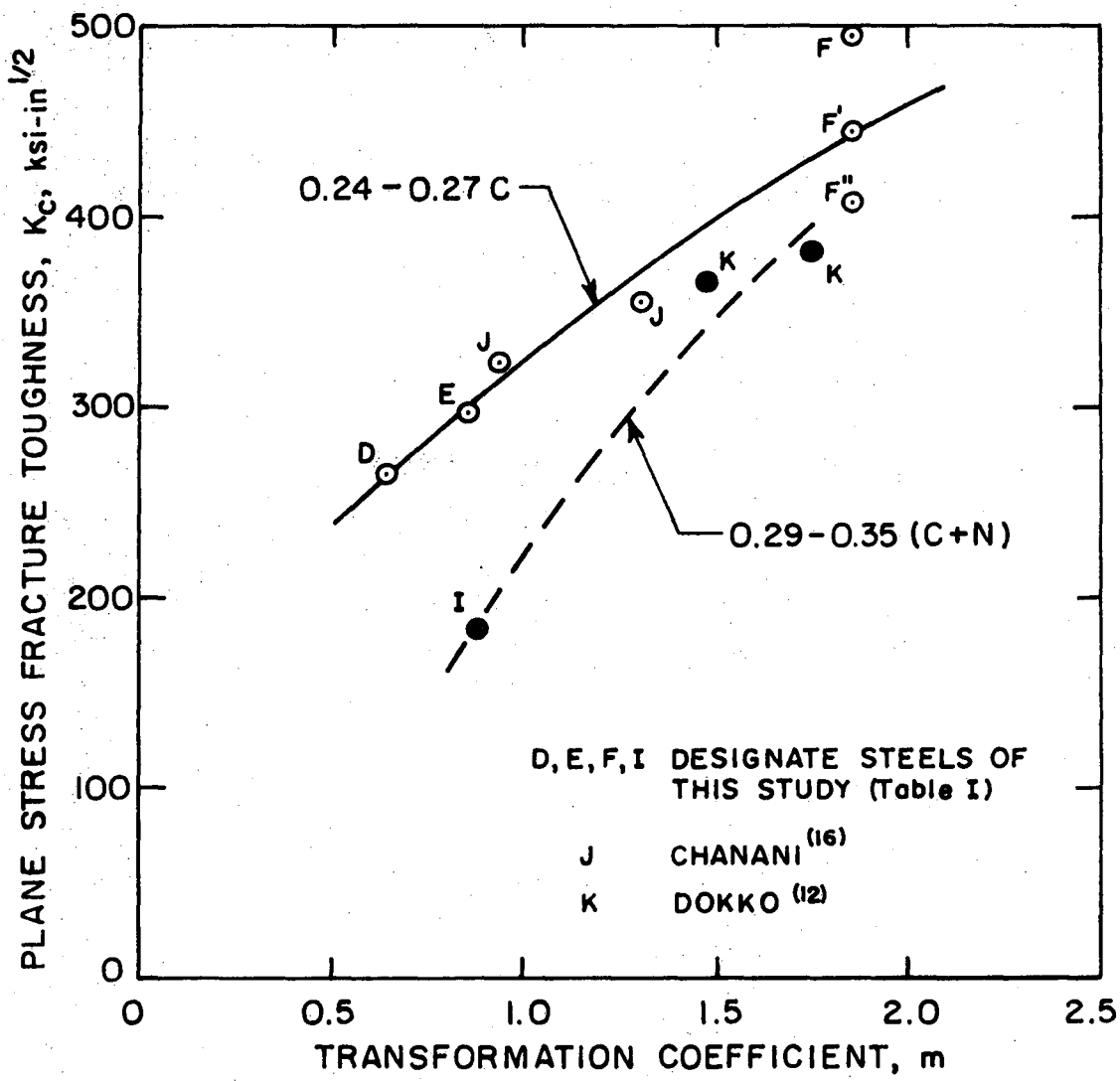

XBL 7011-6952

Fig. 14

LEGAL NOTICE

This report was prepared as an account of Government sponsored work. Neither the United States, nor the Commission, nor any person acting on behalf of the Commission:

A. Makes any warranty or representation, expressed or implied, with respect to the accuracy, completeness, or usefulness of the information contained in this report, or that the use of any information, apparatus, method, or process disclosed in this report may not infringe privately owned rights; or

B. Assumes any liabilities with respect to the use of, or for damages resulting from the use of any information, apparatus, method, or process disclosed in this report.

As used in the above, "person acting on behalf of the Commission" includes any employee or contractor of the Commission, or employee of such contractor, to the extent that such employee or contractor of the Commission, or employee of such contractor prepares, disseminates, or provides access to, any information pursuant to his employment or contract with the Commission, or his employment with such contractor.

TECHNICAL INFORMATION DIVISION
LAWRENCE RADIATION LABORATORY
UNIVERSITY OF CALIFORNIA
BERKELEY, CALIFORNIA 94720